Bioorganic Chemistry 110 (2021) 104743

Contents lists available at ScienceDirect

Bioorganic Chemistry

journal homepage: www.elsevier.com/locate/bioorg

Design, synthesis and biological evaluation of 2,3-dihydro-[1,4]dioxino [2,3-*f*]quinazoline derivatives as EGFR inhibitors

Xuemei Qin [a,*], Leifu Yang [b], Peng Liu [c], Lifang Yang [d], Linmeng Chen [d], Liming Hu [b], Mingguo Jiang [a,*]

[a] *Guangxi Key Laboratory of Polysaccharide Materials and Modifications, School of Marine Sciences and Biotechnology, Guangxi University for Nationalities, Nanning 530008, China*
[b] *College of Life Science and Chemistry & Beijing Key Laboratory of Environmental and Oncology, Beijing University of Technology, Beijing 100124, China*
[c] *Guangzhou Institute of Biomedicine and Health, Chinese Academy of Science, Guangzhou 510530, China*
[d] *School of Chemistry and Chemical Engineering, Guangxi University for Nationalities, Guangxi Nanning 530008, China*

ARTICLE INFO

Keywords:
EGFR inhibitors
Quinazoline derivatives
Lung cancer
Docking

ABSTRACT

Epidermal growth factor receptor (EGFR) is the most attractive target for drug research in non-small cell lung cancer (NSCLC). The first-generation EGFR tyrosine kinase inhibitors (TKIs) Gefetinib and Elotinib showed good clinical efficacy on lung adenocarcinoma tumors, but almost all patients developed resistance to these inhibitors over time. Quinazoline and quinoline derivatives are common targeted inhibitors of EGFR kinase, and their structural optimization is an important direction for the development of effective targeted anticancer drugs. Based on these facts, a series of heterocyclic 2,3-dihydro-[1,4]dioxino[2,3-*f*]quinazoline derivatives have been designed and synthesized and their structures were confirmed by spectral analyses. The cytotoxic activity of the newly synthesized compounds was evaluated against the human kidney epithelial T293 cell line, normal lung cell lines WI-38, non-small cell lung cancer A549 and NCI-H157 cell lines using MTT. The tested compounds showed an evident anticancer activity against the tested cell lines, especially compound **13c**, which was the most potent anticancer agent with half maximal inhibitory concentrations (IC_{50}) between 8.82 and 10.24 μM. Docking study showed that compound **13b** could be nicely bound to the ATP binding pocket of EGFR. In addition, the inhibitory activity of the target compounds against epidermal growth factor receptor tyrosine kinase (EGFR-TK) was evaluated. Results indicated the ability of the target compounds to inhibit EGFR-TK with half maximal inhibitory concentrations (IC_{50}) in the range of 10.29 nM to 652.3 nM. In view of the reported compound activity, the structure deserves further optimization as cancer treatment agents.

1. Introduction

Non-small cell lung cancer (NSCLC) accounts for approximately 85% of all lung cancer cases and is one of the leading causes of cancer death worldwide [1]. Genetic aberrations in the tyrosine kinase domain of EGFR have been confirmed as one of the key drivers of NSCLC progression [2]. Thus, EGFR has become the most effective and attractive therapeutic targets for NSCLC [2,3].

Gefitinib and erlotinib (Fig. 1) [4], as first-generation ATP-competitive and reversible EGFR inhibitors, have been approved for the treatment of NSCLC patients whose lung tumors harbor somatic EGFR mutations L858R and delE746_A750 [5,6]. Unfortunately, most patients who initially respond to gefitinib or erlotinib develop acquired resistance eventually. Especially a secondary point mutation (T790M) in the EGFR active domain is responsible for approximately half of the clinically acquired drug resistance in NSCLC patients [7,8].

In order to address the drug resistance caused by T790M, several second-generation irreversible EGFR inhibitors were developed such as Afatinib and Canertinib (Fig. 1) [9–11]. Afatinib was approved by the FDA for the treatment of late-stage NSCLC patients with actively mutated EGFR in 2013 [12]. The inhibitor contains electrophilic Michael-acceptor systems that can covalently alkylate the conserved cysteine residue (Cys797) at the lip of the ATP binding cleft of EGFR. However, all the second generation inhibitors lack significant selectivity between EGFR T790M mutants and the wild-type EGFR kinase. The inhibition against wild-type EGFR is thought to be responsible for the

* Corresponding authors.
E-mail addresses: qxmei313@126.com (X. Qin), mzxyjiang@163.com (M. Jiang).

https://doi.org/10.1016/j.bioorg.2021.104743
Received 2 August 2020; Received in revised form 15 December 2020; Accepted 9 February 2021
Available online 18 February 2021

side-effect of skin and gastrointestinal toxicities, which will limit their achievable activity against the T790M mutation in patients [13].

The third generation mutant-selective EGFR inhibitors such as Osimertinib (AZD9291, Fig. 1) and rociletinib (CO-1686, Fig. 1) have emerged as potential therapeutics to block the growth of EGFR T790M positive tumors [14,15]. Unlike the first (gefitinib and erlotinib) and second generation (afatinib) EGFR TKIs, both AZD9291 and CO-1686 have a significantly increased potency for EGFR mutants (including T790M) than for $EGFR^{wt}$ [16]. Despite the high efficacy of the third-generation EGFR TKIs, acquired resistance to CO-1686 and AZD9291 have emerged, and C797S point mutation is the leading mechanism of resistance [17–19]. The tries for overcoming EGFR C797S mutation led to the introduction of the fourth-generation inhibitors to the clinical practice [20]. Nowadays, studies are still ongoing to find more efficient EGFR inhibitors in light of the resistance to the current inhibitors [21–23].

In our previous research, we found that compound **b1** (Fig. 2) showed inhibitory activity against $EGFR^{wt}$ (IC_{50} = 2.0 nM) and $EGFR^{T790M/L858R}$ (IC_{50} = 6.9 nM) [24], indicating that the core structure of dihydro[1,4]dioxino [2,3-*f*]quinazoline has potential use for tyrosine kinase inhibitors. Based on our previous researches and attractiveness of tyrosine kinases as promising targets for the design of new cancer agents, taking erlotinib as the leading compound, it was decided to introduce new dihydro[1,4]dioxino [2,3-*f*]quinazoline derivatives by keeping the core structure of dihydro[1,4]dioxino [2,3-*f*]quinazoline remains unchanged. All the compounds were tested against $EGFR^{WT}$ enzyme. The most active compounds were examined for their anti-proliferative activities and toxicity against a number of cancer cells lines and normal cell lines. A molecular docking of the most active compound was carried out to investigate their binding patterns with the EGFR active pocket.

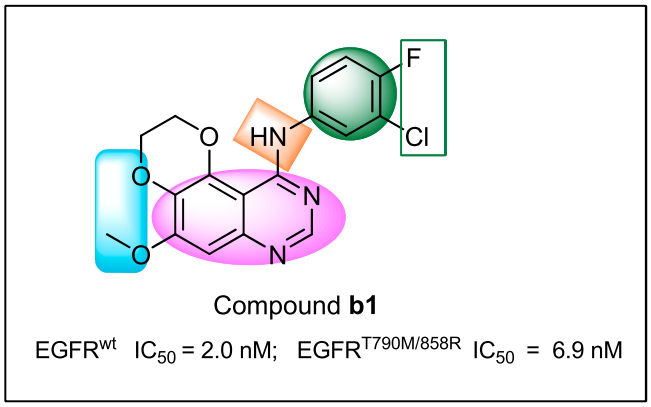

Fig. 2. Our previous compound.

1.1. Rational drug design

The ATP binding pocket of EGFR-TK consists of five main parts; adenine region, hydrophilic ribose pocket, hydrophobic region I, hydrophobic region II and phosphate binding region (Fig. 3) [25–28].

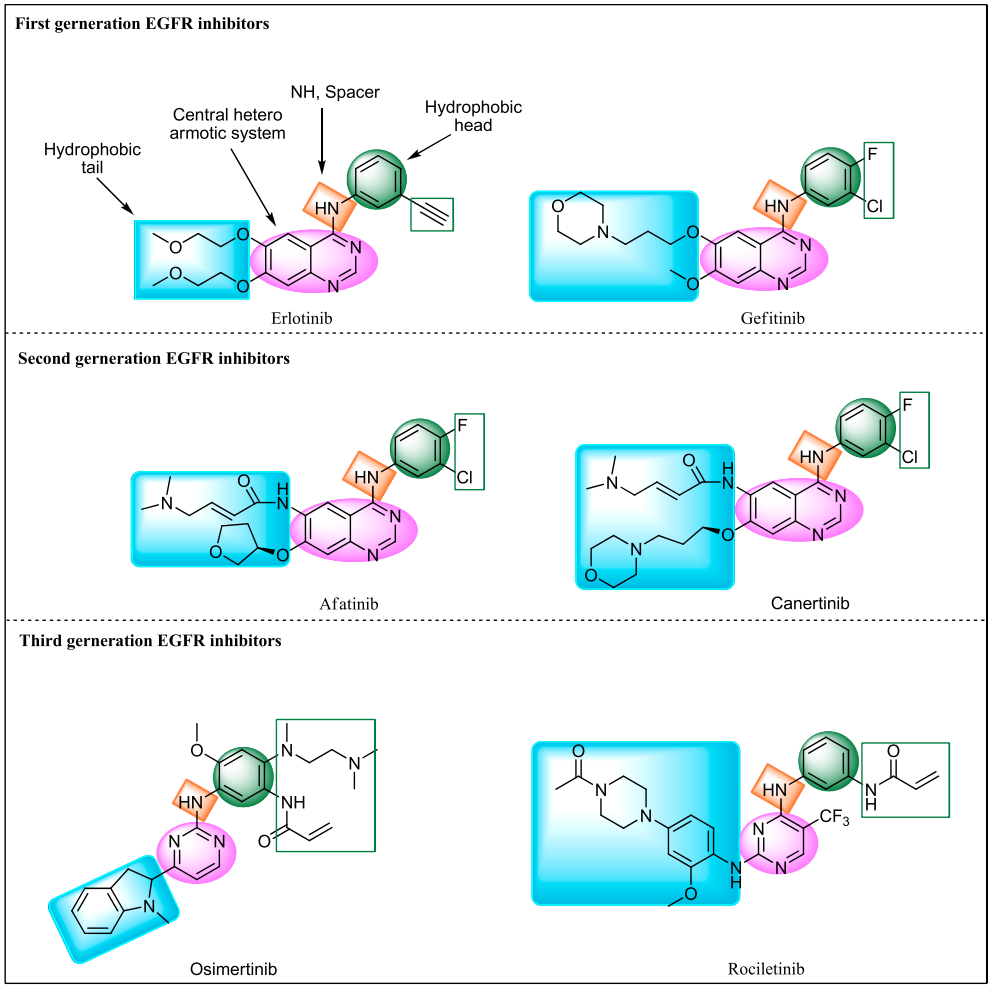

Fig. 1. Basic pharmacophoric features of EGFR-TK inhibitors [4].

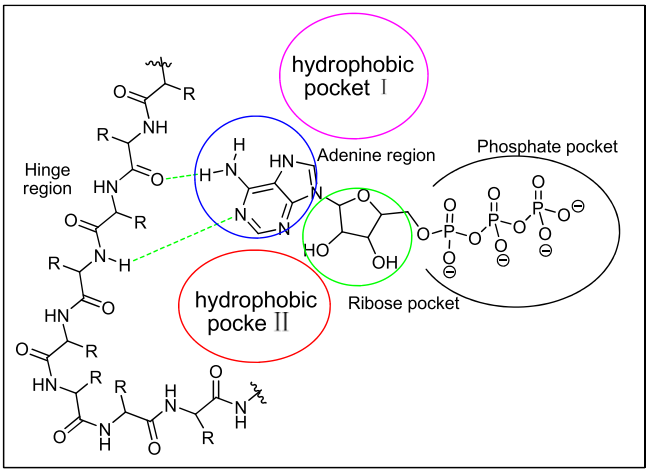

Fig. 3. The ATP binding pocket of EGFR-TK [28].

Nowadays, the EGFR-TKIs do not exploit the ribose and phosphate binding site. Accordingly, the structure-activity relationships (SAR) of majority EGFR-TKIs share four common pharmacophoric features [29], including hydrophobic head, central hetero armotic system, NH spacer, hydrophobic tail as shown in Figs. 1 and 2. The main target of this work was synthesis of new dihydro[1,4]dioxino[2,3-*f*]quinazoline derivatives having the same essential pharmacophoric features of the previous researches and clinically used EGFR-TKIs erlotinib (Fig. 4). The core of our molecular design rational comprised bioisosteric modification strategies of EGFR-TKIs at four different positions.

The first position was the hetero aromatic ring system, where the quinazoline was used the same as erlotinib. One consideration for using the cyclization at 5- and 6-position of the quinazoline is that core cyclization makes the molecule small, thus makes it easier to tolerate the shift of the inhibitors inside the binding pocket due to the mutations, such as T790M. The second position was the terminal hydrophobic head. Diferent hydrophobic substituted phenyl including meta or *para*-position halogen or alkyl substituted phenyl were selected. The third position was the linker (spacer) region, where the linker was NH— the same as the lead compound erlotinib. The fourth position was the hydrophobic tail. Methoxyethyl (compound **13a-13k**) and 3- morpholinopropyl (**14a-14k**) was incorporated to occupy the front hydrophobic region of ATP binding site. All modification pathways and molecular design rationale were illustrated and summarized in Fig. 5.

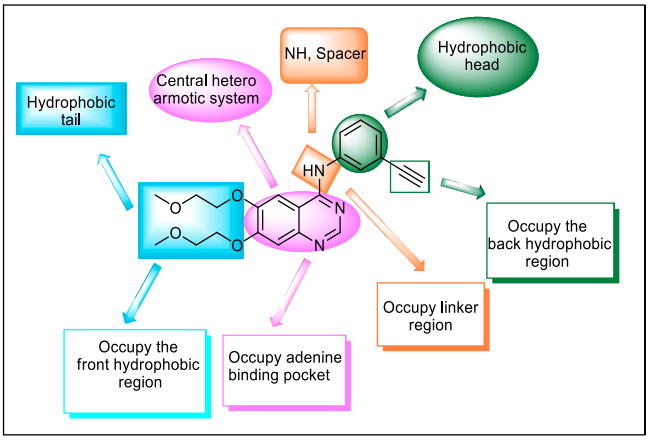

Fig. 4. The basic structural requirements for erlotinib as reported EGFR-TK inhibitor [28].

2. Results and discussion

2.1. Chemistry

Compounds **13a-13k** and **14a-14k** were synthesized according to Scheme 1. The synthesis started with the commercial available 2,3,4-trihydroxybenzoic acid **1**, esterfying with idomethane and $KHCO_3$, to give benzoate **2** in excellent yield. Then intermediate **2** were protected by benzyl and the *ortho*-position benzyl of ester was deprotected selectively by HAc/HCl (10:1) at 40 °C to give **3**. The nucleophilic substitution of compound **3** with epichloro-hydrin resulted in compound **4**, which was then catalyzed by ferric chloride to form compound **5** in methanol. The key intermediate **7** was got by intramolecular cyclization after **6** being chlorination, then reacted with different halogenoalkane to obtain **8**. The intermediate **9** was achieved by selective nitration with the mixture of nitric acid-acetic acid solution. Then catalytic hydrogenation gave **10**, which was subjected to cyclization to generate intermediate **11**, which underwent a nucleophilic **13a-13k** and **14a-14k**.

2.2. Biological activity

2.2.1. Enzyme assay

The newly synthesized [1,4]dioxino[2,3-*f*]quinazoline derivatives were evaluated for their ability to inhibit the autophosphorylation of EGFR kinase using Kinase-Glo luminescent kinase assays. The results were shown in Table 1. The studied compounds displayed inhibition to EGFR kinase with IC_{50} values ranging from 652.3 nM to 10.29 nM. All the compounds displayed significant EGFR inhibitory activities. Among them, compound **13b** showed the most potent inhibitory activity against EGFR kinase (IC_{50} = 10.29 nM), which was comparable to the positive control erlotinib and gefitinib (IC_{50} = 11.65 nM, 10.41 nM, respectively).

To explore the SARs of the novel scaffold, *methoxyethyl* was firstly introduced as R^1 (**13a-13 k**) and the inhibitory activities against EGFR ranged from 10.29 nM to 208.6 nM. When R^3 was hydrogen (**13a**, **13b**, **13c**), compounds substituted by *Cl* or *Br* (**13b**, IC_{50} = 10.29 nM; **13c**, IC_{50} = 15.13 nM) showed excellent potency against EGFR kinase and displayed 6–10 fold increase in potency than substituted by F (**13a**, IC_{50} = 106.1 nM). The reason may be that small fluorine atom could be too small to fill up well the hydrophobic pocket of EGFR kinase pocket. As for bromine atom, its larger volume may not entry into the EGFR pocket well. R^2 or R^3 of the target compounds substituted by methyl (**13k**, IC_{50} = 208.6 nM) or methoxy (**13e**, IC_{50} = 354.7 nM) show weaker activities against EGFR kinase, indicating that grafting a large electron donating group at the 4-positions of quinazoline scaffold is not beneficial for the activity. By comparing **13a** & **13h**, **13b** & **13i** and **13c** & **13j**, it is easy to find the compounds containing meta-substituted aniline showed much more potency against EGFR than compounds containing para-substituted aniline.

To find a more potent EGFR inhibitor, R^1 was substituted by *3-morpholinopropyl* in the subsequent synthesis (**14a-14k**) and the inhibitory activities against EGFR ranged from 13.59 nM to 653.2 nM. By comparing target compounds **13** and **14**, we could conclude that compounds with R^1 being *mothoxyethyl* showed almost the same trend inhibitory efficiency against EGFR as compounds with R^1 being *3-morpholinopropyl* do, indicating that the inhibitory activity of the synthesized compounds depends mainly on the nature of the substituents of aniline. With regard to the un-substituted derivative **14k** (IC_{50} = 321.2 nM), had a lower activity than the substituted ones.

It is important to point ou that when 4-position of quinazoline scaffold are substituted by *3-ethynylphenylamino* (**13d**, **14d**) or *3-chloro-4-fluorophenylamino*, compounds (**13g**, **14g**) showed better inhibitory activity against EGFR. As a whole, compounds substituted by halogens showed better potency against EGFR. The different substituted halogen on aniline, the inhibitory activity of compounds on EGFR was consistent with *Cl* > *Br* > *F* (**13b** > **13c** > **13a**, **14b** > **14c** > **14a**, **13i** > **13j** > **13 h**, **14i** > **14h**).

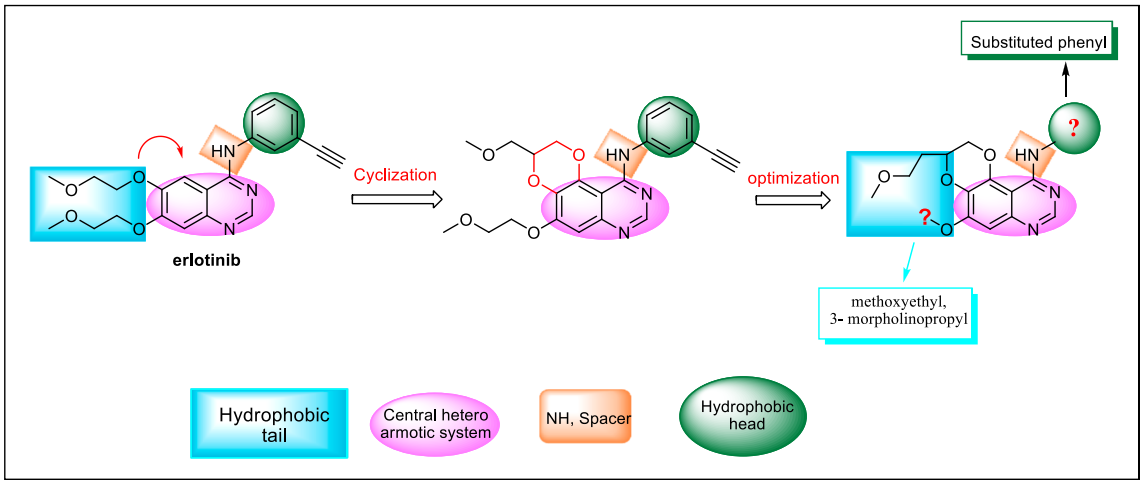

Fig. 5. Rational of molecular design of the new proposed EGFR-TK inhibitors.

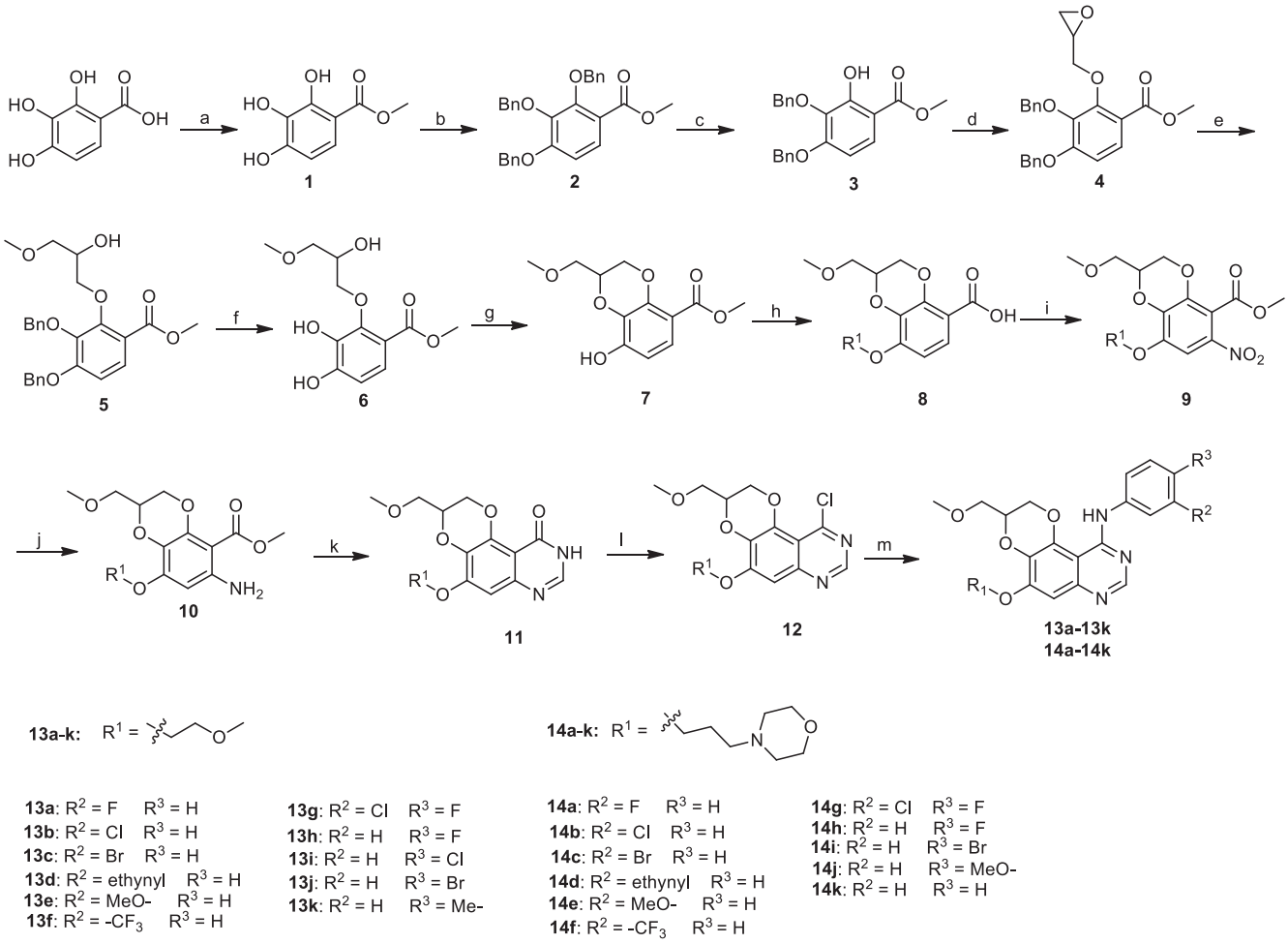

13a-k: R^1 =

14a-k: R^1 =

13a: R^2 = F R^3 = H
13b: R^2 = Cl R^3 = H
13c: R^2 = Br R^3 = H
13d: R^2 = ethynyl R^3 = H
13e: R^2 = MeO- R^3 = H
13f: R^2 = -CF_3 R^3 = H
13g: R^2 = Cl R^3 = F
13h: R^2 = H R^3 = F
13i: R^2 = H R^3 = Cl
13j: R^2 = H R^3 = Br
13k: R^2 = H R^3 = Me-
14a: R^2 = F R^3 = H
14b: R^2 = Cl R^3 = H
14c: R^2 = Br R^3 = H
14d: R^2 = ethynyl R^3 = H
14e: R^2 = MeO- R^3 = H
14f: R^2 = -CF_3 R^3 = H
14g: R^2 = Cl R^3 = F
14h: R^2 = H R^3 = F
14i: R^2 = H R^3 = Br
14j: R^2 = H R^3 = MeO-
14k: R^2 = H R^3 = H

Scheme 1. Reagents and conditions: (a) CH_3I, $KHCO_3$, DMF, 40 °C; (b) BnCl, K_2CO_3, KI, DMF, 60 °C; (c) HCl/H_2O, HAc, 40 °C; (d) epichlorohydrin, Cs_2CO_3, DMF, 70 °C; (e) CH_3OH, $FeCl_3$, rt; (f) Pd/C, H_2, EtOH; (g) $SOCl_2$, DMF, reflux; K_2CO_3, acetone, KI, reflux; (h) R^1-Cl or R^1-Br, K_2CO_3, DMF, 80 °C; (i) HNO_3/HAc; (j) Pd/C, H_2, EtOH; (k) formamidine acetate, EtOH, reflux; (l) $POCl_3$, reflux; (m) anilines, isopropanol, reflux.

2.2.2. *Anti-proliferation assay*

Compounds with better inhibitory activities in enzyme assay were selected to assess for anti-proliferative activity against two non-small cell lung cancer A549 and NCI-H157 cell lines using MTT, using erlotinib as a positive control. The results were showed in Table 2. It is noticeable that almost all the tested compounds demonstrated good activity in blocking tumor cell proliferation compared to the positive control erlotinib.

Table 1
In vitro enzymatic inhibitory activity of compounds **13a-13k** and **14a-14k** against EGFR.[a]

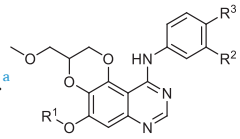

13a-13k & 14a-14k

Compound	R^1	R^2	R^3	IC_{50} (nM)
13a	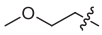	F	H	106.1
13b		Cl	H	10.29
13c	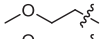	Br	H	15.13
13d	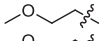	ethynyl	H	39.62
13e	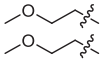	MeO-	H	354.7
13f		$-CF_3$	H	92.89
13g	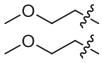	Cl	F	23.1
13h		H	F	164.2
13i	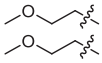	H	Cl	86.79
13j		H	Br	136.3
13k	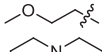	H	Me	208.6
14a	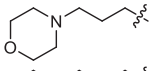	F	H	115.9
14b	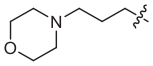	Cl	H	13.59
14c	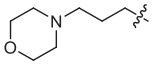	Br	H	15.84
14d	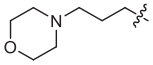	ethynyl	H	37.36
14e	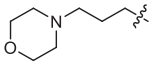	MeO-	H	281.4
14f	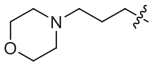	$-CF_3$	H	100.9
14g	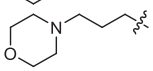	Cl	F	17.6
14h	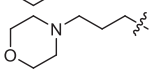	H	F	132.8
14i	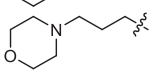	H	Br	90.7
14j	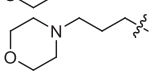	H	MeO-	652.3
14k	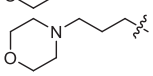	H	H	321.2
gefitinib				10.41
erlotinib				11.65

[a] Values are averages of two independent determinations.

Table 2
Antiproliferative assay *in vitro*.[a]

Compound	A549 IC_{50} (nM)	NCI-H157 IC_{50} (nM)
13b	9.95×10^3	11.66×10^3
13c	8.82×10^3	10.24×10^3
13d	9.23×10^3	19.08×10^3
13g	12.25×10^3	7.76×10^3
14b	19.85×10^3	16.19×10^3
14c	15.21×10^3	16.65×10^3
14d	13.78×10^3	20.89×10^3
14g	13.26×10^3	9.89×10^3
erlotinib	7.29×10^3	6.88×10^3

[a] Values are means of at least two experiment.

2.2.3. Cytotoxicity test

As shown in Table 3, compounds with good inhibitory activities against EGFR kinase were evaluated for their toxicity against the human kidney epithelial T293 cell line and the normal lung cell lines WI-38 using the MTT, these compounds were tested at multiple doses to study the viability of T293 cell and WI-38 cell. The median cytotoxic concentration (CC_{50}) showed that some of the tested compounds did not display any significant cytotoxicity in vitro against T293 cells and WI-38, especially compounds **13b**, **13g** and **14b**.

2.2.4. Docking study

The most active compound **13b** was docked into the three dimensional EGFR active site (1 M17.pdb [30], EGFR/erlotinib crystalline complex) using Autodock software package (version 4.0) with the help of Autodock Tools. In the proposed binding mode, compound **13b** was nicely bound to the ATP binding pocket in a similar manner to erlotinib, showed in Fig. 6**A**. The N-1 of the quinazoline forms an H-bond with the Met769 backbone nitrogen. A water (HOH-10) molecule-mediated hydrogen bonding interaction is observed between quinazoline nitrogen atom (N-3) and other amino acid. The 3-chloro-4-fluoro phenylamino substituent extends into the hydrophobic pocket in the back of the ATP-binding cleft. And compound **13b** was overlaid well with the binding conformation of erlotinib (gray) into the EGFR kinase domain (Fig. 6**B**). The well binding of the inhibitor to the active sites of EGFR may explain its excellent inhibitory activity.

3. Conclusion

In summary, we identified a series of novel [1,4]dioxino[2,3-*f*]quinazoline-based derivates as EGFR inhibitors. All of the compounds showed good inhibitory activities against EGFR kinase ($IC_{50} < 1$ μM). Among them, eight compounds (**13b**, **13c**, **13d**, **13g**, **14b**, **14c**, **14d** and **14g**) showed excellent potency against EGFR kinase, as well as significant anti-proliferative activities against A549 and NCI-H157 cells. Docking study showed that compound **13b** could be nicely bound to the ATP binding pocket of EGFR. It is believed that this work would be helpful for the further research of EGFR inhibitors and expanding the types of compounds that act as EGFR inhibitors.

4. Experiments

4.1. Materials and methods

The reagents were purchased and used without further purification. Melting points were determined on a MP120 melting point apparatus (Hanon instruments Corp., Jinan, China) and are as read. The ^{1}H NMR and ^{13}C NMR spectra were measured on a Bruker 400 MHz Avance or on a Bruker 600 MHz Avance spectrometer with TMS and solvent signals allotted as internal standards. The chemical shifts are reported in ppm (δ). Splitting patterns are designed as s, singlet; d, doublet; t, triplet; m, multiplet. ESI-MS spectra were obtained on an Esquire 6000 Mass

Table 3
The median cytotoxic concentration (CC_{50}) data of texted compounds.[a]

Compound	Cytotoxocity (CC_{50} in nM)	
	T293	WI-38
13b	$>100 \times 10^3$	90.55×10^3
13c	40.10×10^3	70.60×10^3
13d	69.21×10^3	80.64×10^3
13g	82.38×10^3	94.35×10^3
14b	61.50×10^3	100.56×10^3
14c	22.35×10^3	55.37×10^3
14d	38.15×10^3	93.45×10^3
14g	59.16×10^3	45.68×10^3
erlotinib	65.56×10^3	89.38×10^3

[a] Values are means of at least two experiment.

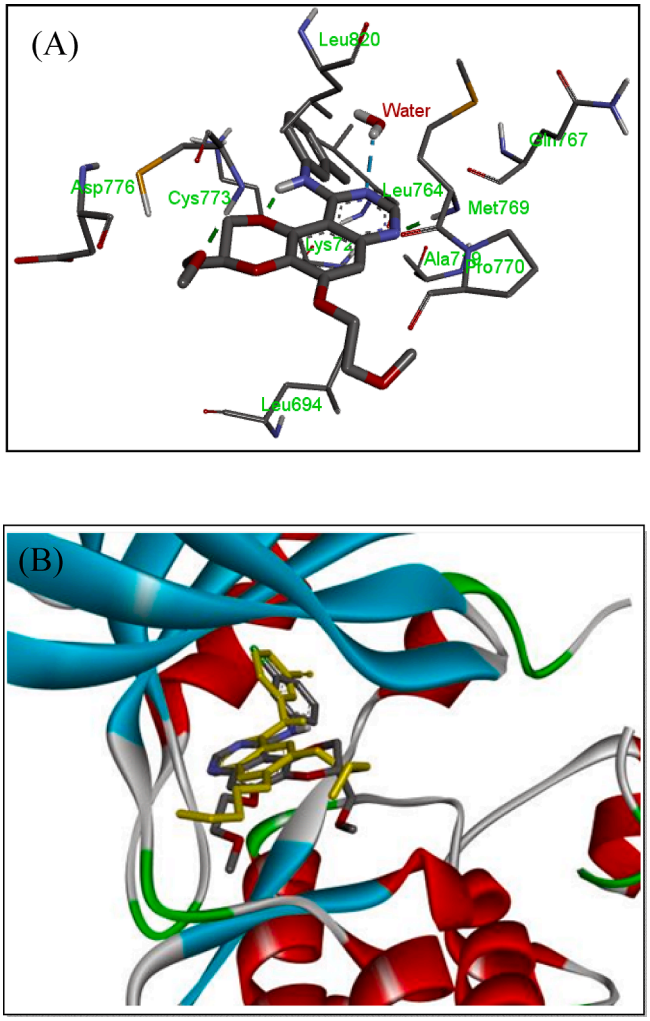

Fig. 6. (A) Binding modes of compound **13b** with the active site of EGFR. (B) Overview of compound **13b** (grey) overlaid with the binding conformation of erlotinib (yellow) into the EGFR active pocket.

Spectrometer. HRMS data were measured using a Bruker APEX IV Fourier transform ion cyclotron resonance mass spectrometer.

4.2. Synthetic procedures

4.2.1. Methyl 2,3,4-trihydroxybenzoate (1)

To a suspension of 2,3,4-trihydroxybenzoic acid (10.0 g, 58.82 mmol) in DMF (150 mL) was added $KHCO_3$ (7.58 g, 70.58 mmol), and the mixture was stirred at room temperature for 10 min, then added CH_3I (5.60 mL, 50.7 mmol). The mixture was heated in water bath at 40 °C and monitored by TLC. After the conversion was completed, the mixture was allowed to cool to room temperature. Then the reaction mixture was poured into 800 mL ice water. The product precipitated as a white solid. Filtration to get the solid and washed with water (70 mL × 4). Product was obtained after drying under vacuum. Yield: 10 g, 92%. ^{1}H NMR (400 MHz, $CDCl_3$) δ 11.01 (s, 1H), 7.38 (d, J = 8.8 Hz, 1H), 6.53 (d, J = 8.8 Hz, 1H), 5.80 (s, 1H), 5.47 (s, 1H), 3.94 (s, 3H). ESI-MS m/z: 183.1 $[M-H]^-$.

4.2.2. Methyl 2,3,4-tris(benzyloxy)benzoate (2)

To a stirred solution of **1** (10 g, 54.30 mmol) in DMF (150 mL) were added K_2CO_3 (37.47 g, 271.5 mmol), KI (0.9 g, 5.4 mmol), followed by benzyl chloride (31.24 mL, 271.5 mmol) and the reaction mixture was heated at 60 °C and monitored by TLC still the reaction completing. The mixture was allowed to cool to room temperature. Then the reaction mixture was poured into 1000 mL ice water. The product precipitated as a white solid. Filtration to get the solid and washed with water and petroleum ether. Product was obtained after drying under vacuum. Yield: 26 g, 95%. ^{1}H NMR (400 MHz, DMSO-d_6) δ 7.28–7.56 (m, 16H), 7.08 (d, J = 8.8 Hz, 1H), 5.23 (d, 2H), 5.00 (d, 4H), 3.76 (s, 3H). ESI-MS m/z: 455.1 $[M + H]^+$.

4.2.3. Methyl 3,4-bis(benzyloxy)-2-hydroxybenzoate (3)

Methyl 2,3,4-tris(benzyloxy)benzoate **2** (10 g, 22 mmol) was dissolved in 550 mL HAc/HCl (V/V, 10:1). The mixture was heated in water bath at 40 °C and monitored by TLC. After the conversion was completed, the reaction mixture was poured into 800 mL ice water. The product precipitated as a white solid. Filtration to get the solid and washed with water. ^{1}H NMR (400 MHz, DMSO-d_6) δ 7.57 (d, J = 9.2 Hz, 1H), 7.29–7.46 (m, 10*H*), 6.80 (d, J = 9.2 Hz, 1H), 5.20 (s, 2H), 4.97 (s, 2H), 3.87 (s, 3H). ESI-MS m/z: 363.0 $[M-H]^-$.

4.2.4. Methyl 3,4-bis(benzyloxy)-2-(oxiran-2-ylmethoxy) benzoate (4)

Cesium carbonate (4.65 g, 14.3 mmol) and epichlorohydrin (1.4 mL, 17.85 mmol) were added to a solution of intermediate **3** (5 g, 11.9 mmol) in DMF. The mixture was heated at 70 °C for 8 h. The reaction was cooled to room temperature, filtered, washed with ethyl acetate, and concentrated, then diluted with water and extracted with ethyl acetate. Organic layer was washed with water and concentrated to oil and separated by chromatographic column on a silica gel to get the product 3.8 g. White solid, yield 75%. ^{1}H NMR (400 MHz, $CDCl_3$) δ 7.64 (d, J = 8.9 Hz, 1H), 7.32–7.48 (m, 10*H*), 6.80 (d, J = 8.9 Hz, 1H), 5.15(s, 2H), 5.06 (q, J = 9.2 Hz, 2H), 4.28 (dd, J = 10.7, 3.6 Hz, 1H), 4.10–4.14 (m, 1H), 3.91 (s, 3H), 3.42 (dt, J = 7.9, 3.2 Hz, 1H), 2.84 (t, J = 4.6 Hz, 1H), 2.65 (dd, J = 5.0, 2.6 Hz, 1H). ESI-MS m/z: 443.2 $[M + Na]^+$.

4.2.5. Methyl 4-(3-c methyl 3,4-bis(benzyloxy)-2-(2-hydroxy-3-methoxy-propoxy)benzoate (5)

A mixture of intermediate **4** (2 g, 4.76 mmol) and anhydr. $FeCl_3$ (0.15 g, 0.96 mmol) in MeOH (50 mL) was stirred at room temperature. The reaction was monitored by TLC. The solvent was removed under vacuum. Water (70 mL) was added and the mixture was extracted with ethyl acetate (2 × 70 mL). The organic solution was dried ($MgSO_4$). Evaporation of the solvent followed by chromatography on a short column of silica gel gave the pure product, 1.4 g. Yellow oil, 65%. ^{1}H NMR (400 MHz, $CDCl_3$) δ 7.67 (d, J = 8.9 Hz, 1H), 7.47–7.35 (m, 7H), 7.35–7.30 (m, 3H), 6.76 (d, J = 8.9 Hz, 1H), 5.13 (d, J = 1.9 Hz, 2H), 5.03 (s, 2H), 4.83 (d, J = 4.0 Hz, 1H), 4.43 (dd, J = 10.2, 2.7 Hz, 1H), 4.22 (dd, J = 10.2, 6.9 Hz, 1H), 4.11 (d, J = 2.4 Hz, 1H), 3.87 (d, J = 1.9 Hz, 3H), 3.51 (d, J = 5.5 Hz, 2H), 3.37 (s, 3H). ESI-MS m/z: 475.3 $[M + Na]^+$.

4.2.6. Methyl 3,4-dihydroxy-2-(2-hydroxy-3-methoxypro-poxy)ben zoate (6)

Intermediate **5** (5.0 g, 11.0 mmol) was dissolved in ethanol (50 mL) followed by the addition of 10% Pd/C (0.2 g). The air was expelled from the vessel, and the mixture was stirred over an atmosphere of hydrogen for 8 h at r.t. The solution was filtered over a bed of celite, and the solvent was evaporated giving a white yellow oil. The product was used for the next step without any purification. ^{1}H NMR (400 MHz, DMSO-d_6) δ 7.96 (s, 2H), 7.16 (d, J = 8.6 Hz, 1H), 6.62 (d, J = 8.6 Hz, 1H), 4.05 (dd, J = 10.1, 3.8 Hz, 1H), 4.01–3.92 (m, 1H), 3.84 (dd, J = 10.0, 6.5 Hz, 1H), 3.75 (s, 3H), 3.72–3.65 (m, 0.5H), 3.41 (ddd, J = 15.9, 10.0, 5.4 Hz, 2H), 3.28 (s, 3H), 3.22 (dd, J = 8.1, 5.5 Hz, 0.5H). ESI-MS m/z: 273.7 $[M + H]^+$.

4.2.7. Methyl 8-hydroxy-2-(methoxymethyl)-2,3-dihydrobenzo [b][1,4] dioxine-5-carboxylate (7)

A suspension of intermediate **6** (2.9 g, 10.7 mmol) in $SOCl_2$ (15 mL) containing 3 drops of DMF was stirred at room temperature for 2 h and

then heated under reflux for 1 h. The $SOCl_2$ was removed under reduced pressure to give crude chloro-substitute. The crude product was dissolved in acetone (50 mL), and then added potassium carbonate (15 g, 107 mmol), KI (0.018 g, 0.11 mmol). The mixture was heated at reflux and the reaction was monitored by TLC still the reaction completing. The reaction was cooled to room temperature, neutralized with HCl at 0 °C and extracted with ethyl acetate. The organic solution was dried ($MgSO_4$). Evaporation of the solvent followed by chromatography on a short column of silica gel gave the pure product, 1.77 g. White solid, 65%. ^{1}H NMR (400 MHz, $CDCl_3$) δ 7.45 (d, J = 8.7 Hz, 1H), 6.55 (d, J = 8.7 Hz, 1H), 4.47–4.38 (m, 2H), 4.16–4.09 (m, 1H), 3.85 (s, 3H), 3.67 (ddd, J = 14.9, 10.5, 5.0 Hz, 2H), 3.43 (s, 3H), 2.14 (s, 1H). ESI-MS *m/z*: 277.1 $[M + Na]^+$.

*4.2.8. General procedure for the preparation of compounds **8a** and **8b***

Intermediate **7** (9.6 mmol), corresponding halogenoalkane (12.5 mmol), and potassium carbonate (28.9 mmol) were stirred in 200 mL acetone at 80 °C for 8 h. The reaction was cooled to room temperature, filtered, concentrated, and purified by silica gel chromatography to afford the product.

*4.2.8.1. Methyl 8-(2-methoxyethoxy)-2-(methoxymethyl)-2,3-dihydrobenzo[b][1,4]dioxine-5-carboxylate **(8a)***. Yellow liquid, yield 88%. ^{1}H NMR (400 MHz, $CDCl_3$) δ 7.46 (d, J = 8.8 Hz, 1H), 6.54 (d, J = 8.9 Hz, 1H), 4.46 (dd, J = 11.4, 1.9 Hz, 1H), 4.39 (dd, J = 11.8, 5.9 Hz, 1H), 4.21 (t, J = 4.9 Hz, 2H), 4.15 (dd, J = 11.3, 7.1 Hz, 1H), 3.87 (s, 3H), 3.80 (t, J = 4.7 Hz, 2H), 3.73 (dd, J = 10.4, 4.8 Hz, 1H), 3.66 (dd, J = 10.4, 6.1 Hz, 1H), 3.46 (s, 3H), 3.43 (s, 3H). ESI-MS *m/z*: 335.1 $[M + Na]^+$.

*4.2.8.2. Methyl 2-(methoxymethyl)-8-(3-morpholinopropoxy)-2,3-dihydrobenzo[b][1,4]-dioxine-5-carboxylate **(8b)***. Yellow liquid, yield 88%. ESI-MS *m/z*: 382.3 $[M + H]^+$.

*4.2.9. General procedure for the preparation of compounds **9a** and **9b***

To a suspension of intermediate **8** (7 mmol) dissolved in AcOH (16 mL) at 0 °C was slowly added fumic HNO_3/HAc (4 mL/12 mL). Then stir at room temperature still the reaction completing and poured into ice water (500 mL). After stirring for 30 min, the resulting precipitate was filtered off, washed with ice water and dried to obtain the nitro compound **9** as a yellow solid.

*4.2.9.1. Methyl 8-(2-methoxyethoxy)-2-(methoxymethyl)-6-nitro-2,3-dihydrobenzo[b][1,4]-dioxine-5-carboxylate **(9a)***. Yellow solid, 83%. ^{1}H NMR (400 MHz, $CDCl_3$) δ 7.43 (s, 1H), 4.42 (t, J = 9.6 Hz, 2H), 4.24 (t, J = 4.5 Hz, 2H), 4.15 (dd, J = 11.5, 7.1 Hz, 1H), 3.95 (s, 3H), 3.80 (d, J = 2.0 Hz, 2H), 3.74 (dd, J = 10.4, 4.6 Hz, 1H), 3.67 (dd, J = 10.4, 6.1 Hz, 1H), 3.45 (s, 3H), 3.42 (s, 3H). ESI-MS *m/z*: 380.2 $[M + Na]^+$.

*4.2.9.2. Methyl 2-(methoxymethyl)-8-(3-morpholinopropoxy)-6-nitro-2,3-dihydrobenzo[b][1,4]dioxine-5-carboxylate **(9b)***. Yellow solid, 83%. ^{1}H NMR (400 MHz, $CDCl_3$) δ 7.40 (s, 1H), 4.40 (dd, J = 8.5, 3.7 Hz, 2H), 4.16 (dd, J = 12.9, 6.8 Hz, 3H), 3.95 (s, 3H), 3.76–3.68 (m, 6H), 3.42 (s, 3H), 2.53 (t, J = 7.0 Hz, 2H), 2.48 (s, 4H), 2.08–1.99 (m, 2H). ESI-MS *m/z*: 427.2 $[M + H]^+$.

*4.2.10. General synthesis method of compounds **10***

To a stirred suspension of intermediate **9** (4.7 mmol) in acetic acid (15 mL) was added zinc powder (1.2 g, 18.8 mmol) and the mixture was heated at 60 °C for 3 h. The reation was cooled to room temperature and then filtered through a celite bed. The filtrate was concentrated and the residue was diluted with EtOAc and washed with water (2 × 100 mL) and dried over anhydrous magnesium sulfate. The solvent was evaporated to give the product as brown oil.

*4.2.10.1. Methyl 6-amino-8-(2-methoxyethoxy)-2-(methoxy- methyl)-2,3-dihydrobenzo[b][1,4]dioxine-5-carboxylate **(10a)***. Brown oily liquid, 90%. ^{1}H NMR (400 MHz, $CDCl_3$) δ 5.76 (s, 1H), 4.27 (dd, J = 11.2, 1.9 Hz, 1H), 4.21–4.13 (m, 1H), 3.96 (dt, J = 11.3, 6.1 Hz, 3H), 3.76 (s, 3H), 3.68–3.62 (m, 2H), 3.58 (dd, J = 10.3, 4.8 Hz, 1H), 3.52 (dd, J = 10.4, 5.9 Hz, 1H), 3.33 (s, 3H), 3.31 (s, 3H).

*4.2.10.2. Methyl 6-amino-2-(methoxymethyl)-8-(3-morpholino propoxy)-2,3-dihydrobenzo[b][1,4]-dioxine-5-carboxylate **(10b)***. Brown oily liquid, 90%. ESI-MS *m/z*: 397.4 $[M + H]^+$.

*4.2.11. General synthesis method of compounds **11***

A mixture of **10** (20 mmol) and formamidine acetate (24 mmol) in ethanol (60 mL) was heated at reflux for 5 h. The mixture was cooled and filtered. The precipitate was washed with ethanol and dried to afford the product.

*4.2.11.1. 5-(2-methoxyethoxy)-3-(methoxymethyl)-2,3-dihydro-[1,4]dioxino[2,3-f]quinazolin-10(9H)-one **(11a)***. White solid; Yield: 69%. ^{1}H NMR (400 MHz, $CDCl_3$) δ 11.80 (s, 1H), 7.99 (s, 1H), 6.85 (s, 1H), 4.60 (dd, J = 11.4, 2.2 Hz, 1H), 4.47–4.37 (m, 1H), 4.34–4.20 (m, 3H), 3.84 (dd, J = 7.1, 4.7 Hz, 2H), 3.74 (qd, J = 10.5, 5.3 Hz, 2H), 3.47 (s, 3H), 3.44 (s, 3H). ESI-MS *m/z*: 320.8 $[M + H]^+$.

*4.2.11.2. 3-(methoxymethyl)-5-(3-morpholino-propoxy)-2,3-dihydro[1,4]dioxino[2,3-f]quinazolin-10(9H)-one **(11b)***. White solid; Yield: 70%. ^{1}H NMR (400 MHz, DMSO-d_6) δ 11.78 (s, 1H), 7.85 (s, 1H), 6.76 (s, 1H), 4.44–4.32 (m, 2H), 4.14 (t, J = 6.4 Hz, 2H), 4.04 (dd, J = 11.2, 7.0 Hz, 1H), 3.64–3.55 (m, 6H), 2.40 (dd, J = 18.0, 10.9 Hz, 6H), 1.91 (p, J = 6.6 Hz, 2H).

*4.2.12. General synthesis method of compounds **12***

A mixture of intermediate **11** (7.0 mmol) and $POCl_3$ (15 mL) was heated at reflux temperature for 3 h. The solvent were removed under reduced pressure. The residue was dissolved in CH_2Cl_2 (50 mL) and the organic layer was washed with cold aqueous $NaHCO_3$ solution and brine, and dried over $MgSO_4$, filtered and evaporated to give the product.

*4.2.12.1. 10-chloro-5-(2-methoxyethoxy)-3-(methoxymethyl)-2,3-dihydro-[1,4]dioxino[2,3-f]quinazoline **(12a)***. White solid; Yield: 72%. ^{1}H NMR (400 MHz, $CDCl_3$) δ 8.78 (s, 1H), 7.06 (s, 1H), 4.55 (dd, J = 11.4, 2.3 Hz, 1H), 4.52–4.45 (m, 1H), 4.34 (t, J = 4.1 Hz, 2H), 4.25 (dd, J = 11.4, 6.8 Hz, 1H), 3.92–3.85 (m, 2H), 3.76 (ddd, J = 16.5, 10.4, 5.4 Hz, 2H), 3.48 (d, J = 7.9 Hz, 6H). ESI-MS *m/z*: 341.3 $[M + H]^+$.

*4.2.12.2. 10-chloro-3-(methoxymethyl)-5-(3-morpholinopropoxy) −2,3-dihydro-[1,4]dioxino[2,3-f]quinazoline **(12b)***. White solid; Yield:75%. ESI-MS *m/z*: 410.3 $[M + H]^+$.

*4.2.13. General synthesis method of compounds **13** & **14***

A mixture of 4-chloroquinazolines derivatives **12** (5 mmol) and substituted anilines (6 mmol) in isopropanol (25 mL) was stirred at reflux for 3 h. The reaction mixture was cooled to room temperature and the resultant precipitate was collected by filtration. The solid was further dried in vacuum to give the product.

*4.2.13.1. N-(3-fluorophenyl)-5-(2-methoxyethoxy)-3-(methoxy-methyl)-2,3-dihydro-[1,4]dioxino[2,3-f]quinazolin-10-amine **(13a)***. White solid; Yield: 58%; mp: 231.6–232.2 °C. ^{1}H NMR (500 MHz, CD_3OD + $CDCl_3$) δ 8.58 (s, 1H), 7.63 (dt, J = 10.3, 2.2 Hz, 1H), 7.48–7.37 (m, 2H), 7.11 (s, 1H), 7.09–7.01 (m, 1H), 4.83 (dd, J = 11.4, 2.2 Hz, 1H), 4.55–4.50 (m, 1H), 4.44 (dd, J = 11.4, 7.5 Hz, 1H), 4.38 (t, J = 4.4 Hz, 2H), 3.88 (dd, J = 7.2, 3.7 Hz, 2H), 3.82 (qd, J = 10.7, 4.9 Hz, 2H), 3.47 (d, J = 1.5 Hz, 6H). ^{13}C NMR (125 MHz, CD_3OD + $CDCl_3$) δ 162.67, 158.18, 156.41,

148.41, 139.59, 137.34, 134.53, 133.55, 130.20, 119.49, 113.67, 111.41, 99.30, 94.35, 72.00, 70.23, 70.17, 69.50, 66.87, 59.19, 58.75. HRMS (ESI) *m/z*: 416.1622 calcd for $C_{21}H_{22}FN_3O_5$, $[M + H]^+$, found 416.1624. HPLC purity: 100%.

4.2.13.2. N-(3-chlorophenyl)-5-(2-methoxyethoxy)-3-(methoxy-methyl)-2,3-dihydro-[1,4]dioxino[2,3-f]quinazolin-10-amine ***(13b)***. White solid; Yield: 62%; mp: 233.3–234.7 °C. ^{1}H NMR (500 MHz, $CD_3OD + CDCl_3$) δ 8.59 (s, 1H), 7.82 (s, 1H), 7.56 (d, $J = 8.0$ Hz, 1H), 7.43 (t, $J = 8.1$ Hz, 1H), 7.33 (d, $J = 8.0$ Hz, 1H), 7.14 (s, 1H), 4.84 (dd, $J = 11.3$, 1.7 Hz, 1H), 4.54 (d, [1]$J = 5.0$ Hz, 1H), 4.45 (dd, $J = 11.3$, 7.5 Hz, 1H), 4.40 (t, $J = 4.3$ Hz, 2H), 3.92–3.87 (m, 2H), 3.83 (qd, $J = 10.8$, 4.8 Hz, 2H), 3.49 (d, $J = 0.9$ Hz, 6H). ^{13}C NMR (125 MHz, $CD_3OD + CDCl_3$) δ 158.25, 156.45, 148.37, 139.62, 137.08, 134.47, 134.42, 133.54, 130.02, 126.96, 124.22, 122.33, 99.25, 94.26, 72.02, 70.25, 70.17, 69.52, 66.87, 59.19, 58.75. HRMS (ESI) *m/z*: 432.1326 calcd for $C_{21}H_{22}ClN_3O_5$ $[M + H]^+$, found 432.1329. HPLC purity: 100%.

4.2.13.3. N-(3-bromophenyl)-5-(2-methoxyethoxy)-3-(methoxy-methyl)-2,3-dihydro-[1,4]dioxino[2,3-f]quinazolin-10-amine ***(13c)***. White solid; Yield: 70%; mp: 239.1–241.7 °C. ^{1}H NMR (500 MHz, $CD_3OD + CDCl_3$) δ 8.59 (s, 1H), 7.95 (t, $J = 1.8$ Hz, 1H), 7.63–7.58 (m, 1H), 7.48 (dd, $J =$ 8.0, 0.8 Hz, 1H), 7.38 (t, $J = 8.1$ Hz, 1H), 7.13 (s, 1H), 4.84 (dd, $J = 11.4$, 2.1 Hz, 1H), 4.57–4.52 (m, 1H), 4.45 (dd, $J = 11.4$, 7.5 Hz, 1H), 4.40 (t, $J = 4.3$ Hz, 2H), 3.89 (dd, $J = 6.9$, 3.7 Hz, 2H), 3.83 (qd, $J = 10.7$, 4.8 Hz, 2H), 3.49 (d, $J = 0.8$ Hz, 6H). ^{13}C NMR (125 MHz, $CD_3OD + CDCl_3$) δ 158.26, 156.46, 148.37, 139.62, 137.17, 134.42, 133.55, 130.27, 129.94, 127.10, 122.83, 122.23, 99.24, 94.25, 72.01, 70.24, 70.17, 69.52, 66.86, 59.20, 58.76. HRMS (ESI) *m/z*: 476.0816 calcd for $C_{21}H_{22}BrN_3O_5$ $[M + H]^+$, found 476.0819. HPLC purity: 100%.

4.2.13.4. N-(3-ethynylphenyl)-5-(2-methoxyethoxy)-3-(methoxy-methyl)-2,3-dihydro-[1,4]dioxino[2,3-f]quinazolin-10-amine ***(13d)***. White solid; Yield: 50%; mp: 238.1–239.3 °C. ^{1}H NMR (500 MHz, $CD_3OD + CDCl_3$) δ 8.56 (s, 1H), 7.82 (d, $J = 0.9$ Hz, 1H), 7.69–7.64 (m, 1H), 7.46–7.41 (m, 2H), 7.14 (s, 1H), 4.84 (dd, $J = 11.4$, 2.1 Hz, 1H), 4.57–4.53 (m, 1H), 4.45 (dd, $J = 11.4$, 7.5 Hz, 1H), 4.40 (t, $J = 4.3$ Hz, 2H), 3.89 (dd, $J =$ 6.9, 3.6 Hz, 2H), 3.83 (qd, $J = 10.8$, 4.9 Hz, 2H), 3.49 (s, 6H), 3.38 (s, 1H). ^{13}C NMR (125 MHz, $CD_3OD + CDCl_3$) δ 158.26, 156.36, 148.34, 139.64, 136.00, 134.37, 133.48, 130.48, 129.04, 127.47, 124.58, 123.25, 99.19, 94.26, 82.23, 78.48, 72.01, 70.25, 70.16, 69.50, 66.85, 59.20, 58.75. HRMS (ESI) *m/z*: 422.1716 calcd for $C_{23}H_{23}N_3O_5$ $[M + H]^+$, found 422.1720. HPLC purity: 99.27%.

4.2.13.5. 5-(2-methoxyethoxy)-3-(methoxymethyl)-N-(3-methoxy-phenyl)-2,3-dihydro-[1,4]dioxino-[2,3-f]quinazolin-10-amine ***(13e)***. White solid; Yield: 85%; mp: 233.0–233.7 °C. ^{1}H NMR (500 MHz, $CD_3OD + CDCl_3$) δ 8.54 (s, 1H), 7.39 (t, $J = 8.2$ Hz, 1H), 7.31 (t, $J = 2.2$ Hz, 1H), 7.28 (s, 1H), 7.17 (dd, $J = 8.0$, 1.3 Hz, 1H), 6.91 (dd, $J = 8.1$, 2.1 Hz, 1H), 4.80 (dd, $J = 11.3$, 2.1 Hz, 1H), 4.53 (dt, $J = 6.7$, 3.6 Hz, 1H), 4.45 (dd, $J = 11.3$, 7.4 Hz, 1H), 4.41 (t, $J = 4.3$ Hz, 2H), 3.90–3.78 (m, 7H), 3.49 (s, 6H). ^{13}C NMR (125 MHz, $CD_3OD + CDCl_3$) δ 160.15, 158.13, 156.21, 148.28, 139.33, 136.70, 134.47, 133.41, 129.91, 116.08, 112.43, 110.14, 99.15, 94.69, 71.75, 70.16, 70.12, 69.52, 66.93, 59.43, 58.92, 55.30. HRMS (ESI) *m/z*: 428.1822 calcd for $C_{22}H_{25}N_3O_6$ $[M + H]^+$, found 428.1830. HPLC purity: 100%.

4.2.13.6. 5-(2-methoxyethoxy)-3-(methoxymethyl)-N-(3-(trifluoro methyl)phenyl)-2,3-dihydro-[1,4]dioxino[2,3-f]quinazolin-10-amine ***(13f)***. White solid; Yield: 45%; mp: 232.3–233.0 °C. ^{1}H NMR (500 MHz, $CD_3OD + CDCl_3$) δ 8.60 (s, 1H), 8.05 (s, 1H), 7.89 (d, $J = 7.8$ Hz, 1H), 7.63 (dt, $J = 24.5$, 8.7 Hz, 2H), 7.14 (s, 1H), 4.85 (dd, $J = 11.4$, 2.2 Hz, 1H), 4.58–4.53 (m, 1H), 4.46 (dd, $J = 11.4$, 7.5 Hz, 1H), 4.41 (t, $J = 4.4$ Hz, 2H), 3.90 (dd, $J = 7.2$, 3.7 Hz, 2H), 3.84 (qd, $J = 10.8$, 4.9 Hz, 2H), 3.49 (d, $J = 1.5$ Hz, 6H). ^{13}C NMR (125 MHz, $CD_3OD + CDCl_3$) δ 158.45, 156.54, 148.42, 139.67, 136.60, 134.51, 133.58, 131.21, 129.65, 127.73, 123.61, 123.44, 121.15, 99.29, 94.25, 72.04, 70.25, 70.17, 69.53, 66.85, 59.19, 58.75. HRMS (ESI) *m/z*: 466.1590 calcd for $C_{22}H_{22}F_3N_3O_5$ $[M + H]^+$, found 466.1596. HPLC purity: 100%.

4.2.13.7. N-(4-chloro-3-fluorophenyl)-5-(2-methoxyethoxy)-3-(methoxymethyl)-2,3-dihydro-[1,4]dioxino[2,3-f]quinazolin-10-amine ***(13g)***. Light yellow solid; Yield: 60%; mp: 248.2–250.5 °C. ^{1}H NMR (500 MHz, $CD_3OD + CDCl_3$) δ 8.57 (s, 1H), 7.86 (dd, $J = 6.5$, 2.6 Hz, 1H), 7.58–7.54 (m, 1H), 7.29 (t, $J = 8.7$ Hz, 1H), 7.13 (s, 1H), 4.83 (dd, $J = 11.4$, 2.1 Hz, 1H), 4.56–4.51 (m, 1H), 4.44 (dd, $J = 11.4$, 7.5 Hz, 1H), 4.40 (t, $J = 4.3$ Hz, 2H), 3.89 (dd, $J = 7.2$, 3.7 Hz, 2H), 3.83 (qd, $J = 10.8$, 4.9 Hz, 2H), 3.49 (d, $J = 1.9$ Hz, 6H). ^{13}C NMR (125 MHz, $CD_3OD + CDCl_3$) δ 158.40, 156.53, 155.53, 148.38, 139.66, 134.44, 133.52, 132.57, 126.78, 124.57, 121.08, 116.68, 99.17, 94.26, 72.00, 70.24, 70.17, 69.52, 66.82, 59.21, 58.77. HRMS (ESI) *m/z*: 450.1232 calcd for $C_{21}H_{21}ClFN_3O_5$ $[M + H]^+$, found 450.1235. HPLC purity: 95.33%.

4.2.13.8. N-(4-fluorophenyl)-5-(2-methoxyethoxy)-3-(methoxy-methyl)-2,3-dihydro-[1,4]dioxino[2,3-f]quinazolin-10-amine ***(13h)***. Light yellow solid; Yield: 55%; mp: 239.3–240.9 °C. ^{1}H NMR (500 MHz, $CD_3OD + CDCl_3$) δ 8.51 (s, 1H), 7.67–7.61 (m, 2H), 7.22–7.16 (m, 2H), 7.10 (s, 1H), 4.82 (dd, $J = 11.4$, 2.2 Hz, 1H), 4.56–4.51 (m, 1H), 4.44 (dd, $J =$ 11.4, 7.5 Hz, 1H), 4.40 (t, $J = 4.4$ Hz, 2H), 3.89 (dd, $J = 7.2$, 3.7 Hz, 2H), 3.83 (qd, $J = 10.8$, 4.9 Hz, 2H), 3.49 (d, $J = 2.4$ Hz, 6H). ^{13}C NMR (125 MHz, $CD_3OD + CDCl_3$) δ 162.17, 158.41, 156.26, 148.41, 139.75, 134.42, 133.38, 131.84, 126.41, 115.84, 115.66, 99.12, 94.29, 71.96, 70.26, 70.18, 70.26, 69.45, 66.80, 59.20, 58.76. HRMS (ESI) *m/z*: 416.1622 calcd for $C_{21}H_{22}FN_3O_5$ $[M + H]^+$, found 416.1625. HPLC purity: 100%.

4.2.13.9. N-(4-chlorophenyl)-5-(2-methoxyethoxy)-3-(methoxy-methyl)-2,3-dihydro-[1,4]dioxino[2,3-f]quinazolin-10-amine ***(13i)***. White solid; Yield: 61%; mp: 247.1–247.8 °C. ^{1}H NMR (500 MHz, $CD_3OD + CDCl_3$) δ 8.55 (s, 1H), 7.68–7.63 (m, 2H), 7.48–7.43 (m, 2H), 7.12 (s, 1H), 4.83 (dd, $J = 11.4$, 2.2 Hz, 1H), 4.56–4.51 (m, 1H), 4.45 (dd, $J = 11.4$, 7.5 Hz, 1H), 4.40 (t, $J = 4.4$ Hz, 2H), 3.89 (dd, $J = 7.3$, 3.7 Hz, 2H), 3.83 (qd, J = 10.7, 4.8 Hz, 2H), 3.49 (d, $J = 2.1$ Hz, 6H). ^{13}C NMR (125 MHz, $CD_3OD + CDCl_3$) δ 158.22, 156.37, 148.33, 139.66, 134.49, 134.36, 133.48, 132.45, 129.02, 125.58, 99.22, 94.24, 71.99, 70.24, 70.17, 69.49, 66.84, 59.20, 58.76. HRMS (ESI) *m/z*: 432.1326 calcd for $C_{21}H_{22}ClN_3O_5$ $[M + H]^+$, found 432.1330. HPLC purity: 100%.

4.2.13.10. N-(4-bromophenyl)-5-(2-methoxyethoxy)-3-(methoxy-methyl)-2,3-dihydro-[1,4]dioxino[2,3-f]quinazolin-10-amine ***(13j)***. White solid; Yield: 74%; mp: 240.4–242.4 °C. ^{1}H NMR (500 MHz, $CD_3OD + CDCl_3$) δ 8.55 (s, 1H), 7.60 (s, 4H), 7.11 (s, 1H), 4.83 (dd, $J =$ 11.4, 2.2 Hz, 1H), 4.56–4.51 (m, 1H), 4.45 (dd, $J = 11.4$, 7.5 Hz, 1H), 4.40 (t, $J = 4.4$ Hz, 2H), 3.89 (dd, $J = 7.3$, 3.7 Hz, 2H), 3.83 (qd, $J =$ 10.7, 4.8 Hz, 2H), 3.49 (d, $J = 1.9$ Hz, 6H). ^{13}C NMR (125 MHz, CD_3OD + $CDCl_3$) δ 158.15, 156.36, 148.35, 139.64, 135.02, 134.43, 133.49, 132.01, 125.81, 120.21, 99.26, 94.28, 71.99, 70.24, 70.17, 69.49, 66.84, 59.20, 58.76. HRMS (ESI) *m/z*: 476.0821 calcd for $C_{21}H_{22}BrN_3O_5$ $[M + H]^+$, found 476.0821. HPLC purity: 100%.

4.2.13.11. 5-(2-methoxyethoxy)-3-(methoxymethyl)-N-p-tolyl-2,3-dihydro-[1,4]dioxino[2,3-f]quinazolin-10-amine ***(13k)***. White solid; Yield: 85%; mp: 233.0–233.7 °C. ^{1}H NMR (500 MHz, $CD_3OD + CDCl_3$) δ 8.54 (s, 1H), 7.39 (t, $J = 8.2$ Hz, 1H), 7.31 (t, $J = 2.2$ Hz, 1H), 7.28 (s, 1H), 7.17 (dd, $J = 8.0$, 1.3 Hz, 1H), 6.91 (dd, $J = 8.1$, 2.1 Hz, 1H), 4.80 (dd, J = 11.3, 2.1 Hz, 1H), 4.53 (dt, $J = 6.7$, 3.6 Hz, 1H), 4.45 (dd, $J = 11.3$, 7.4 Hz, 1H), 4.41 (t, $J = 4.3$ Hz, 2H), 3.90–3.78 (m, 7H), 3.49 (s, 6H). ^{13}C NMR (125 MHz, $CD_3OD + CDCl_3$) δ 160.15, 158.13, 156.21, 148.28, 139.33, 136.70, 134.47, 133.41, 129.91, 116.08, 112.43, 110.14, 99.15, 94.69, 71.75, 70.16, 70.12, 69.52, 66.93, 59.43, 58.92, 55.30, 0.75.

HRMS (ESI) *m/z*: 428.1872 calcd for $C_{22}H_{25}N_3O_6$ [M + H]$^+$, found 428.1879. HPLC purity: 100%.

4.2.13.12. N-(3-fluorophenyl)-3-(methoxymethyl)-5-(3-morpholino propoxy)-2,3-dihydro-[1,4]dioxino[2,3-f] quinazolin-10-amine ***(14a)***. White solid; Yield: 65%; mp: 125.0–125.9 °C. ^{1}H NMR (400 MHz, $CDCl_3$ + CD_3OD) δ 9.44 (s, 1H), 8.58 (s, 1H), 7.86 (d, J = 11.3 Hz, 1H), 7.34 (q, J = 7.5 Hz, 2H), 6.97 (d, J = 9.2 Hz, 1H), 6.83 (t, J = 7.5 Hz, 1H), 4.65 (d, J = 11.0 Hz, 1H), 4.56–4.45 (m, 1H), 4.38 (dd, J = 11.1, 6.9 Hz, 1H), 4.23 (t, J = 6.4 Hz, 2H), 3.82 (dd, J = 10.3, 4.6 Hz, 1H), 3.75 (dd, J = 8.6, 5.2 Hz, 5H), 2.55 (dd, J = 21.4, 14.2 Hz, 6H), 2.10 (p, J = 6.7 Hz, 2H). ^{13}C NMR (125 MHz, $CDCl_3$ + CD_3OD) δ 163.09, 156.49, 153.91, 153.38, 146.84, 140.58, 137.76, 131.40, 129.83, 116.63, 110.25, 108.82, 102.52, 101.51, 71.41, 70.50, 67.46, 67.04, 66.38, 59.72, 55.35, 53.77, 26.02. HRMS (ESI) *m/z*: 485.2200 calcd for $C_{25}H_{29}FN_4O_5$ [M + H]$^+$, found 485 0.2193. HPLC purity: 100%.

4.2.13.13. N-(3-chlorophenyl)-3-(methoxymethyl)-5-(3-morpholinopropoxy)-2,3-dihydro-[1,4]dioxino[2,3-f] quinazolin-10-amine ***(14b)***. White solid; Yield: 78%; mp: 149.0–150.8. ^{1}H NMR (400 MHz, $CDCl_3$ + CD_3OD) δ 9.38 (s, 1H), 8.57 (s, 1H), 7.93 (s, 1H), 7.61 (d, J = 8.2 Hz, 1H), 7.37–7.22 (m, 1H), 7.09 (d, J = 7.3 Hz, 1H), 6.96 (d, J = 8.4 Hz, 1H), 4.64 (d, J = 10.9 Hz, 1H), 4.54–4.44 (m, 1H), 4.38 (dd, J = 11.1, 6.9 Hz, 1H), 4.22 (t, J = 6.5 Hz, 2H), 3.78 (ddd, J = 13.9, 9.0, 4.4 Hz, 6H), 3.48 (s, 3H), 2.54 (dd, J = 21.3, 14.1 Hz, 6H), 2.10 (p, J = 6.7 Hz, 2H). ^{13}C NMR (125 MHz, $CDCl_3$ + CD_3OD) δ 156.41, 153.84, 153.33, 146.77, 140.13, 137.68, 134.43, 131.35, 129.76, 123.54, 121.39, 119.41, 102.44, 101.42, 71.35, 70.45, 67.39, 66.98, 66.32, 59.65, 55.29, 53.71, 25.96. HRMS (ESI) *m/z*: 501.1905 calcd for $C_{25}H_{29}ClN_4O_5$ [M + H]$^+$, found 501.1892. HPLC purity: 95.63%.

4.2.13.14. N-(3-bromophenyl)-3-(methoxymethyl)-5-(3-morpho- lino propoxy)-2,3-dihydro-[1,4]dioxino-[2,3-f]quinazolin-10-amine ***(14c)***. White solid; Yield: 80%; mp: 139.4–141.2 °C. ^{1}H NMR (400 MHz, $CDCl_3$ + CD_3OD) δ 9.37 (s, 1H), 8.57 (s, 1H), 8.04 (s, 1H), 7.70 (d, J = 1.1 Hz, 1H), 7.25 (d, J = 4.6 Hz, 2H), 6.96 (d, J = 8.8 Hz, 1H), 4.65 (d, J = 11.0 Hz, 1H), 4.55–4.45 (m, 1H), 4.38 (dd, J = 11.1, 6.9 Hz, 1H), 4.23 (t, J = 6.5 Hz, 2H), 3.78 (ddd, J = 13.8, 8.9, 4.4 Hz, 6H), 3.49 (s, 3H), 2.55 (dd, J = 21.3, 14.1 Hz, 6H), 2.10 (p, J = 6.7 Hz, 2H). ^{13}C NMR (125 MHz, $CDCl_3$ + CD_3OD) δ 156.40, 153.86, 153.34, 146.77, 140.27, 137.68, 131.35, 130.08, 126.49, 124.24, 122.46, 119.95, 102.44, 101.42, 71.36, 70.44, 67.40, 66.97, 66.33, 59.66, 55.29, 53.70, 25.96. HRMS (ESI) *m/z*: 545.1400 calcd for $C_{25}H_{29}BrN_4O_5$ [M + H]$^+$, found 545.1403. HPLC purity: 100%.

4.2.13.15. N-(3-ethynylphenyl)-3-(methoxymethyl)-5-(3-morpholinopropoxy)-2,3-dihydro-[1,4]dioxino[2,3-f] quinazolin-10-amine ***(14d)***. White solid; Yield: 59%; mp: 112.1–113.7 °C. ^{1}H NMR (400 MHz, $CDCl_3$ + CD_3OD) δ 9.35 (s, 1H), 8.55 (s, 1H), 7.84 (d, J = 9.9 Hz, 2H), 7.34 (t, J = 7.8 Hz, 1H), 7.24 (s, 1H), 6.95 (d, J = 9.4 Hz, 1H), 4.63 (d, J = 11.2 Hz, 1H), 4.49 (d, J = 5.6 Hz, 1H), 4.37 (dd, J = 11.1, 6.8 Hz, 1H), 4.21 (t, J = 6.4 Hz, 2H), 4.02 (d, J = 5.5 Hz, 1H), 3.84–3.66 (m, 6H), 3.47 (s, 3H), 2.53 (dd, J = 21.4, 14.2 Hz, 6H), 2.17–2.00 (m, 2H). ^{13}C NMR (125 MHz, $CDCl_3$ + CD_3OD) δ 155.59, 152.99, 152.31, 145.78, 137.98, 136.80, 130.31, 127.93, 126.45, 123.94, 121.68, 121.25, 101.44, 100.47, 82.52, 70.38, 69.47, 66.42, 66.01, 65.31, 58.69, 54.33, 52.74, 24.99. HRMS (ESI) *m/z*: 491.2294 calcd for $C_{27}H_{30}N_4O_5$ [M + H]$^+$, found 491.2293. HPLC purity: 100%.

4.2.13.16. 3-(methoxymethyl)-N-(3-methoxyphenyl)-5-(3-morpholinopropoxy)-2,3-dihydro-[1,4]dioxino-[2,3-f] quinazolin-10-amine ***(14e)***. White solid; Yield: 67%; mp: 127.6–128.1 °C. ^{1}H NMR (400 MHz, $CDCl_3$ + CD_3OD) δ 9.36 (s, 1H), 8.55 (s, 1H), 7.57 (s, 1H), 7.31 (d, J = 8.1 Hz, 1H), 7.21 (d, J = 7.9 Hz, 1H), 6.96 (d, J = 9.2 Hz, 1H), 6.71 (d, J = 7.0 Hz, 1H), 4.63 (d, J = 10.5 Hz, 1H), 4.50 (d, J = 6.4 Hz, 1H), 4.37 (dd, J = 11.1, 6.8 Hz, 1H), 4.23 (t, J = 6.5 Hz, 2H), 3.87 (s, 3H), 3.85–3.71 (m, 6H), 3.49 (s, 3H), 2.55 (dd, J = 21.4, 14.2 Hz, 6H), 2.19–2.04 (m, 2H). ^{13}C NMR (125 MHz, $CDCl_3$ + CD_3OD) δ 160.13, 156.70, 154.08, 153.16, 146.71, 140.02, 137.87, 131.17, 129.50, 114.03, 109.22, 107.89, 102.37, 101.51, 71.32, 70.46, 67.36, 66.98, 66.25, 59.65, 55.32, 55.31, 53.70, 25.97. HRMS (ESI) *m/z*: 497.2400 calcd for $C_{26}H_{32}N_4O_6$ [M + H]$^+$, found 497.2349. HPLC purity: 99.64%.

4.2.13.17. 3-(methoxymethyl)-5-(3-morpholino-propoxy)-N-(3-(trifluoromethyl)phenyl)-2,3-dihydro-[1,4]dioxino[2,3-f]quinazolin-10-amine ***(14f)***. White solid; Yield: 52%; mp: 130.6–134.4 °C. ^{1}H NMR (400 MHz, $CDCl_3$ + CD_3OD) δ 9.47 (s, 1H), 8.58 (s, 1H), 8.03 (d, J = 8.4 Hz, 2H), 7.51 (t, J = 7.7 Hz, 1H), 7.38 (d, J = 7.6 Hz, 1H), 6.99 (d, J = 9.6 Hz, 1H), 4.68 (d, J = 11.0 Hz, 1H), 4.51 (d, J = 6.0 Hz, 1H), 4.40 (dd, J = 11.0, 6.9 Hz, 1H), 4.24 (t, J = 6.4 Hz, 2H), 3.83 (dd, J = 10.2, 4.6 Hz, 1H), 3.75 (dd, J = 10.6, 6.3 Hz, 5H), 3.49 (s, 3H), 2.57 (t, J = 7.1 Hz, 2H), 2.50 (s, 4H), 2.12 (dd, J = 13.6, 6.8 Hz, 2H). ^{13}C NMR (125 MHz, $CDCl_3$ + CD_3OD) δ 156.52, 153.88, 153.48, 146.90, 139.54, 137.74, 131.49, 131.31, 129.37, 124.66, 123.30, 120.13, 118.15, 102.55, 101.47, 71.45, 70.52, 67.48, 67.04, 66.45, 59.72, 55.35, 53.77, 26.03. HRMS (ESI) *m/z*: 535.2168 calcd for $C_{26}H_{29}F_3N_4O_5$ [M + H]$^+$, found 535.2170. HPLC purity: 96.48%.

4.2.13.18. N-(3-chloro-4-fluorophenyl)-3-(methoxymethyl)-5-(3-morpholinopropoxy)-2,3-dihydro-[1,4]dioxino[2,3-f] quinazolin-10-amine ***(14g)***. White solid; Yield: 59%; mp: 158.7–160.8 °C. ^{1}H NMR (400 MHz, $CDCl_3$ + CD_3OD) δ 9.28 (s, 1H), 8.55 (s, 1H), 7.95 (d, J = 4.3 Hz, 1H), 7.60–7.53 (m, 1H), 7.16 (t, J = 8.8 Hz, 1H), 6.97 (d, J = 9.5 Hz, 1H), 4.65 (d, J = 11.2 Hz, 1H), 4.50 (d, J = 5.0 Hz, 1H), 4.38 (dd, J = 11.0, 6.9 Hz, 1H), 4.23 (t, J = 6.4 Hz, 2H), 3.82 (dd, J = 10.2, 4.6 Hz, 1H), 3.75(dd, J = 8.9, 5.2 Hz, 5H), 3.49 (s, 3H), 2.57 (t, J = 7.1 Hz, 2H), 2.50 (s, 4H), 2.17–2.05 (m, 2H). ^{13}C NMR (125 MHz, $CDCl_3$ + CD_3OD) δ 156.55, 153.90, 153.50, 146.81, 137.76, 135.55, 131.42, 123.87, 121.47, 120.91, 116.56, 116.38, 102.52, 101.33, 71.41, 70.49, 67.48, 67.04, 66.41, 59.72, 55.35, 53.77, 26.02. HRMS (ESI) *m/z*: 519.1811 calcd for $C_{25}H_{28}ClFN_4O_5$ [M + H]$^+$, found 519.1812. HPLC purity: 95.80%.

4.2.13.19. N-(4-fluorophenyl)-3-(methoxymethyl)-5-(3-morpholino propoxy)-2,3-dihydro-[1,4]dioxino[2,3-f]quinazolin-10-amine ***(14h)***. White solid; Yield: 63%; mp: 122.3–123.4 °C. ^{1}H NMR (400 MHz, $CDCl_3$ + CD_3OD) δ 9.24 (s, 1H), 8.51 (s, 1H), 7.68 (dd, J = 8.7, 4.8 Hz, 2H), 7.10 (t, J = 8.6 Hz, 2H), 6.95 (d, J = 9.4 Hz, 1H), 4.63 (d, J = 11.0 Hz, 1H), 4.50 (d, J = 6.0 Hz, 1H), 4.37 (dd, J = 11.1, 6.8 Hz, 1H), 4.23 (t, J = 6.5 Hz, 2H), 3.81 (dd, J = 10.2, 4.6 Hz, 1H), 3.75 (t, J = 6.6 Hz, 5H), 3.49 (s, 3H), 2.57 (t, J = 7.1 Hz, 2H), 2.49 (s, 4H), 2.17–2.04 (m, 2H). ^{13}C NMR (125 MHz, $CDCl_3$ + CD_3OD) δ 156.86, 154.26, 154.07, 153.23, 146.69, 137.91, 134.69, 131.18, 123.91, 123.85, 115.64, 115.46, 102.37, 101.31, 71.32, 70.45, 67.38, 66.98, 66.28, 59.65, 55.30, 53.71, 25.97. HRMS (ESI) *m/z*: 485.2200 calcd for $C_{25}H_{29}FN_4O_5$ [M + H]$^+$, found 485.2200. HPLC purity: 100%.

4.2.13.20. N-(4-bromophenyl)-3-(methoxymethyl)-5-(3-morpholino propoxy)-2,3-dihydro-[1,4]dioxino[2,3-f]quinazolin-10-amine ***(14i)***. White solid; Yield: 85%; mp: 169.8–172.3 °C. ^{1}H NMR (400 MHz, $CDCl_3$ + CD_3OD) δ 9.29 (d, J = 32.7 Hz, 1H), 8.54 (s, 1H), 7.67 (d, J = 8.6 Hz, 2H), 7.50 (d, J = 8.7 Hz, 2H), 6.96 (d, J = 9.1 Hz, 1H), 4.64 (d, J = 10.9 Hz, 1H), 4.55–4.45 (m, 1H), 4.37 (dd, J = 11.1, 6.9 Hz, 1H), 4.23 (t, J = 6.5 Hz, 2H), 3.81 (dd, J = 10.2, 4.6 Hz, 1H), 3.74 (t, J = 6.5 Hz, 5H), 3.49 (s, 3H), 2.55 (dd, J = 21.4, 14.2 Hz, 6H), 2.10 (p, J = 6.8 Hz, 2H). ^{13}C NMR (125 MHz, $CDCl_3$ + CD_3OD) δ 156.53, 153.94, 153.36, 146.81, 138.02, 137.79, 131.85, 131.36, 123.33, 116.30, 102.49, 101.49, 71.39, 70.51, 67.45, 67.04, 66.38, 59.72, 55.35, 53.77, 26.03. HRMS (ESI) *m/z*: 547.1379 calcd for $C_{25}H_{29}BrN_4O_5$ [M + H]$^+$, found 547.1366. HPLC purity: 100%.

4.2.13.21. 3-(methoxymethyl)-N-(4-methoxy phenyl)-5-(3-morpholin opropoxy)-2,3-dihydro-[1,4]dioxino[2,3-f]quinazolin-10-amine ***(14j)***. White solid; Yield: 65%; mp: 129.8–131.3 °C. ^{1}H NMR (400 MHz, $CDCl_3$ + CD_3OD) δ 9.14 (s, 1H), 8.48 (s, 1H), 7.58 (d, J = 8.6 Hz, 2H), 7.02–6.88 (m, 3H), 4.61 (d, J = 10.8 Hz, 1H), 4.49 (d, J = 6.4 Hz, 1H), 4.36 (dd, J = 11.1, 6.8 Hz, 1H), 4.22 (t, J = 6.4 Hz, 2H), 3.88–3.77 (m, 4H), 3.75 (d, J = 3.9 Hz, 5H), 3.48 (s, 3H), 2.54 (dd, J = 21.3, 14.2 Hz, 6H), 2.22–2.02 (m, 2H). ^{13}C NMR (125 MHz, $CDCl_3$ + CD_3OD) δ 157.17, 156.53, 154.33, 153.06, 146.61, 138.08, 131.59, 130.99, 124.22, 114.21, 102.29, 101.33, 71.31, 70.48, 67.34, 66.98, 66.21, 59.64, 55.50, 55.31, 53.70, 25.98. HRMS (ESI) *m/z*: 497.2400 calcd for $C_{26}H_{32}N_4O_6$ $[M + H]^+$, found 497.2391. HPLC purity: 95.84%.

4.2.13.22. 3-(methoxymethyl)-5-(3-morpholino-propoxy)-N-phenyl-2,3-dihydro-[1,4]dioxino[2,3-f]quinazolin-10-amine ***(14k)***. White solid; Yield: 78%; mp: 128.0–129.7 °C. ^{1}H NMR (400 MHz, $CDCl_3$ + CD_3OD) δ 9.35 (s, 1H), 8.54 (s, 1H), 7.75 (d, J = 7.9 Hz, 2H), 7.41 (t, J = 7.7 Hz, 2H), 7.15 (t, J = 7.2 Hz, 1H), 6.96 (d, J = 9.2 Hz, 1H), 4.63 (d, J = 10.8 Hz, 1H), 4.50 (d, J = 5.4 Hz, 1H), 4.37 (dd, J = 11.1, 6.8 Hz, 1H), 4.23 (t, J = 6.4 Hz, 2H), 3.87–3.68 (m, 6H), 3.49 (s, 3H), 2.55 (dd, J = 21.5, 14.3 Hz, 6H), 2.10 (p, J = 6.7 Hz, 2H). ^{13}C NMR (125 MHz, $CDCl_3$ + CD_3OD) δ 156.83, 154.19, 153.22, 146.79, 138.84, 137.99, 131.21, 128.97, 124.00, 121.93, 102.44, 101.54, 71.39, 70.53, 67.42, 67.05, 66.31, 59.71, 55.37, 53.77, 26.04. HRMS (ESI) *m/z*: 467.2294 calcd for $C_{25}H_{30}N_4O_6$ $[M + H]^+$, found 467.2293. HPLC purity: 98.78%.

4.3. EGFR inhibitory assay

Kinase-Glo luminescent kinase assay is a homogeneous non-radioactive method for determining the activity of purified kinases by quantifying the amount of ATP remaining in solution following a kinase reaction. Target compounds and positive compound gefitinib were dissolved in DMSO as 10 mM stock solution, then diluted it to 100 μM with DMSO and transferred to the dose plate. The compounds was serially diluted with DMSO in 5-fold. Then each concentration was diluted 10-fold with reaction buffer (containing 25 mM HEPES, 10 mM $MgCl_2$, 100 μg/mL BSA, 0.01% TritonX-100, 2.5 mM DTT and adjusted pH to 7.4) to obtain a 10 × final concentration. Transferred compounds with its concentration ranging from 10 μM to 0.0006 μM to assay plate for EGFR activity test with a volume of 1 μL/well. For HPE (hundred percent effect: No kinase and no compound, but containing ATP, substrate and 1% DMSO) and ZPE (zero percent effect: No compound but containing kinase, ATP, substrate and 1% DMSO) well, diluted 2 μL DMSO 10-fold with reaction buffer to obtain 10% DMSO solution. Then transferred it to the assay plat, 1 μL/well. Procedure for kinase reaction is: 1) Add 10 × compound to the assay plate in a 384-well plate layout, 1 μL/well. For the HPE and ZPE wells, equal volume (1 μL/well) of 10% DMSO was added to the 384-well assay plate; 2) Added 2.5 × kinase EGFR into the assay plate as 384-well plate layout, 4 μL/well. For HPE wells, an equal volume (4 μL/well) of assay buffer was added to the 384-well assay plate; 3) Centrifuged the assay plate with 1000 rpm for 1 min to mix them; 4) Pre-incubated the assay plate at 30℃ for 30 min; 5) Mixed equal volume of 4 × ATP and 4 × substrate to obtain 2 × ATP-substrate mixtures; 6) Added 2 × ATP-substrate mixture to the assay plate, 5 μL/well; 7) Centrifuged the assay plate at 1000 rpm for 1 min to mix; 8) Incubated the plate for one hour at 30 °C; 9) Kinase glo plus was added to each well (10 μL/well), and then incubated the assay plate for 20 min at 27 °C; 10) Read luminescence signal with Envision. The raw data were analysed by Prism 5.0 and the inhibitory rate was calculated by the following formula: Compound inhibitory rate = ("compound" reading-ZPE)/(HPE-ZPE) × 100%.

4.4. The anti-proliferative and cytotoxicity activity

The anti-proliferative and cytotoxicity activity was determined using MTT assay (Dojindo, Japan). Cells lines were seeded at a density of 3000 cells/well in 96-well microtiter plates and were incubated at 37 °C overnight in a humidified incubator containing 5% CO_2. Cells were dosed with compounds at final concentrations ranging from 0.025 to 80 μM in each well of the plate. After 48 h, 50 μL of the MTT solution was added and incubated for 4 h. Cell survival was determined by measuring the absorbance at 492 nm using a microplate reader. A calibration curve was prepared using the data obtained from the wells that contain known numbers of viable cells to determine the IC_{50} of the target compounds.

4.5. Docking study

The molecular docking of compound **13b** into the three-dimensional EGFR complex structure (PDB code: 1 M17.pdb, downloaded from the PDB) was performed using CDocker. Unwanted water and ligands were removed by the DS4.0. The structures of the molecules were drawn by Gaussian 03 software, then optimized the molecules to the minimum energy conformation used the semi-empirical AM1 method. Docking procedure was performed by AutoDock 4.0 software with the help of Autodock Tools. Tutorials may be found at: http://autodock.scripps.edu/faqs-help/tutorial.

4.5.1. EGFR binding pocket model building

The EGFR binding pocket model was generated by Discovery Studio 4.0 (DS4.0) based on the crystal structure of EGFR/erlotinib. Unwanted water and ligands were removed by the DS4.0 to build the initial receptor structure for docking.

4.5.2. Small molecular preparation

The small molecular structure of **13b** was drawn by Gaussian03 software, then optimized the molecules to the minimum energy conformation used the semi-empirical AM1 method.

4.5.3. Docking protocol

Docking procedure was performed by AutoDock 4 software with the help of Autodock Tools. The grid maps were calculated using AutoGrid4 for three dockings, a grid map with 60 × 70 × 60 points and a grid-point spacing of 0.375 Å was applied. In order to fully explore the possible binding conformations, 100 conformations were generated using the Lamarckian Genetic Algorithm (LGA). For other docking parameters, standard values were used as software default. Cluster analysis was performed on the results using a root mean square (RMS) tolerance of 2.0 Å. The conformations and binding energy for further analysis were obtained from the average of the biggest cluster.

Declaration of Competing Interest

The authors declare that they have no known competing financial interests or personal relationships that could have appeared to influence the work reported in this paper.

Acknowledgments

The authors would like to acknowledge financial support from Scientific Research Project of Guangxi University for Nationalities (2019KJQN005), the Middle-aged and Young Teachers' Basic Ability Promotion Project of Guangxi (2017KY0165), the Talent Introduction Project of Guangxi University for Nationalities (2016MDQD008), and the Science and Technology Major Project of Guangxi (AA18242026).

Appendix A. Supplementary material

Supplementary data to this article can be found online at https://doi.org/10.1016/j.bioorg.2021.104743.

References

[1] R.L. Siegel, K.D. Miller, A. Jemal, CA: A Cancer J. Clinicians 69 (1) (2019) 7–34.
[2] S.V. Sharma, D.W. Bell, J. Settleman, D.A. Haber, Nat. Rev. Cancer 7 (3) (2007) 169–181.
[3] J. Huang, J. Huang, N. Wang, L. Wang, G. Huang, Bioorg. Chem. 89 (2019), 102994.
[4] A.A. Gaber, A.H. Bayoumi, A.M. El-morsy, F.F. Sherbiny, A.B.M. Mehany, I. H. Eissa, Bioorg. Chem. 80 (2018) 375–395.
[5] T.J. Lynch, D.W. Bell, R. Sordella, S. Gurubhagavatula, D.A. Haber, N. Engl. J. Med. 350 (21) (2004) 2129–2139.
[6] J.G. Paez, P.A. Janne, J.C. Lee, S. Tracy, H. Greulich, S. Gabriel, P. Herman, F.J. Kaye, N. Lindeman, T.J. Boggon, K. Naoki, H. Sasaki, 7.Y. Fujii, M.J. Eck, W.R. Sellers, B.E. Johnson, M. Meyerson, Science 304(5676) (2004) 1497–1500.
[7] A. Passaro, E. Guerini-Rocco, A. Pochesci, D. Vacirca, G. Spitaleri, C.M. Catania, A. Rappa, M. Barberis, F. de Marinis, Pharmacol. Res. 117 (2017) 406–415.
[8] C.R. Chong, P.A. Janne, Nat. Med. 19 (11) (2013) 1389–1400.
[9] E.L. Kwak, S. Raffaella, D.W. Bell, G.H. Nadia, R.A. Okimoto, B.W. Brannigan, P. L. Harris, D.R. Driscoll, F. Panos, T.J. Lynch, Proc. Natl. Acad. Sci. 102 (21) (2005) 7665–7670.
[10] J.A. Engelman, K. Zejnullahu, C.M. Gale, E. Lifshits, A.J. Gonzales, T. Shimamura, F. Zhao, P.W. Vincent, G.N. Naumov, J.E. Bradner, I.W. Althaus, L. Gandhi, G. I. Shapiro, J.M. Nelson, J.V. Heymach, M. Meyerson, K.K. Wong, P.A. Janne, Cancer Res. 67 (24) (2007) 11924–11932.
[11] D. Li, L. Ambrogio, T.S. Kubo, M. Takahashi, L. Chirieac, R. Padera, G. Shapiro, A. Baum, F. Himmelsbach, W. Rettig, Oncogene 27(34) (2008) 4702–4711.
[12] R.T. Dungo, G.M. Keating, Drugs 73 (13) (2013) 1503–1515.
[13] J.B. Johnston, S. Navaratnam, M.W. Pitz, J.M. Maniate, E. Wiechec, H. Baust, J. Gingerich, G.P. Skliris, L.C. Murphy, M. Los, Curr. Med. Chem. 13 (29) (2006) 3483–3492.
[14] D.A. Cross, S.E. Ashton, S. Ghiorghiu, C. Eberlein, C.A. Nebhan, P.J. Spitzler, J. P. Orme, M.R. Finlay, R.A. Ward, M.J. Mellor, G. Hughes, A. Rahi, V.N. Jacobs, M. Red Brewer, E. Ichihara, J. Sun, H. Jin, P. Ballard, K. Al-Kadhimi, R. Rowlinson, T. Klinowska, G.H. Richmond, M. Cantarini, D.W. Kim, M.R. Ranson, W. Pao, Cancer Discoverv 4 (9) (2014) 1046–1061.
[15] A.O. Walter, R.T. Sjin, H.J. Haringsma, K. Ohashi, J. Sun, K. Lee, A. Dubrovskiy, M. Labenski, Z. Zhu, Z. Wang, M. Sheets, T. St Martin, R. Karp, D. van Kalken, P. Chaturvedi, D. Niu, M. Nacht, R.C. Petter, W. Westlin, K. Lin, S. Jaw-Tsai, M. Raponi, T. Van Dyke, J. Etter, Z. Weaver, W. Pao, J. Singh, A.D. Simmons, T. C. Harding, A. Allen, Cancer Discoverv 3 (12) (2013) 1404–1415.
[16] P. Zofia, M.J. Niederst, C.A. Karlovich, H.A. Wakelee, J.W. Neal, M.K. Mari, F. Linnea, A.N. Hata, E.L. Lockerman, K. Anuj, Cancer Discovery 5 (7) (2015) 713–722.
[17] Y.C. Zhang, Z.H. Chen, X.C. Zhang, C.R. Xu, H.H. Yan, Z. Xie, S.K. Chuai, J.Y. Ye, H. Han-Zhang, Z. Zhang, X.Y. Bai, J. Su, B. Gan, J.J. Yan g, W.F. Li, W. Tang, F.R. Luo, X. Xu, Y.L. Wu, Q. Zhou, EBioMedicine 43 (2019) 180–187.
[18] S. Schmid, J.J.N. Li, N.B. Leighl, Lung Cancer 147 (2020) 123–129.
[19] D. Das, L. Xie, J. Wang, J. Shi, J. Hong, Bioorg Chem 99 (2020), 103790.
[20] A. Ayati, S. Moghimi, S. Salarinejad, M. Safavi, B. Pouramiri, A. Foroumadi, Bioorg. Chem. 99 (2020), 103811.
[21] H.A. Allam, E.E. Aly, A.K.B.A.W. Farouk, A. Elkerdawy, S.E.S. Abbass, Bioorg. Chem. 98 (2020), 103726.
[22] R. Nadjet, M.A. Almehmadi, S. Ihmaid, A.M. Shehata, A. Omar, H.E.A. Ahmed, M. R. Aouad, Bioorg. Chem. 103 (2020), 104133.
[23] H. Wei, Y. Duan, W. Gou, J. Cui, H. Ning, D. Li, Y. Qin, Q. Liu, Y. Li, Eur. J. Med. Chem. 181 (2019), 111552.
[24] X. Qin, Z. Li, L. Yang, P. Liu, L. Hu, C. Zeng, Z. Pan, Bioorgan. Med. Chem. 26 (2016) 2871–2881.
[25] V. Gandin, A. Ferrarese, M. Dalla Via, C. Marzano, A. Chilin, G. Marzaro, Sci. Rep. 5 (2015) 16750.
[26] P. Traxler, P. Furet, Pharmacol. Ther. 82 (1999) 195–206.
[27] S.A. Elmetwally, K.F. Saied, I.H. Eissa, E.B. Elkaeed, Bioorg Chem 88 (2019), 102944.
[28] J. Zhang, P.L. Yang, N.S. Gray, Nat. Rev. Cancer 9 (1) (2009) 28–39.
[29] S. Mowafy, A. Galanis, Z.M. Doctor, R.M. Paranal, D.S. Lasheen, N.A. Farag, P. A. Jänne, K.A. Abouzid, Bioorg. Med. Chem. 24 (2016) 3501–3512.
[30] H. Berman, K. Henrick, H. Nakamura, Nat. Struct. Mol. Biol. 10 (2003) 980.